

# A Degenerate Conic-Based Method for a Direct Fitting and 3-D Pose of Cylinders with a Single Perspective View

Christophe Doignon and Michel de Mathelin

**Abstract**—In this paper, we address the problem of the pose recovery of a straight homogeneous circular cylinder (SHCC) from its apparent contour in a single 2-D image. In many real-world situations, one may encounter cylindrical objects especially in man-made structures. Object models based on surfaces of revolution, in particular cylinders, are suitable for many fields, like the automatic assembly, the human motion capture and also in medical image-based robotic guidance. To model the geometry of a SHCC, we first introduce a singular matrix which represents this degenerate quadric and we show it can be expressed with the Plücker coordinates of its symmetry axis. We demonstrate that the perspective projection of a SHCC is related to the pose parameters and for this model-based pose estimation problem, we present a degenerate conic-based fitting method which has some connections with the estimation of the Fundamental matrix. We provide a closed-form solution for the pose determination (4 dof). Compared to earlier works in this field, the proposed approach exhibits some geometric properties of SHCCs, it can deal with partial occlusions of apparent contours and it provides an efficient direct pose solution for the symmetry axis. Simulated data and real images are used to validate the fitting and pose computation. Finally, to highlight the effectiveness of the proposed method to deal with apparent contours in a poor structured environment, we apply this work to the localization of instruments used in laparoscopic surgery.

## I. INTRODUCTION

### A. Motivations

The recovery of the 3-D information from 2-D images is a fundamental problem in computer vision and for the past four decades, the model-based pose estimation has been widely addressed. Monocular scene analysis based on perspective projection can be successfully used to solve the determination of 3-D object attitude if an a priori knowledge is available. The choice of the involved primitives is a key point since they must be robust to noise and efficiently detectable. In the man-made mechanical object recognition field, geometrical features like straight lines, circles or cylinders are often encountered and for cylindrical objects, e.g., food cans, missiles, containers, pipes and circular pillars, quadrics of revolution can be thought as important components for object modeling, tracking or grasping. Such visual cue occurs in many areas like assembly, human motion capture [8], mobile robot guidance and in medical image analysis, e.g. for estimating geometrical transformations between fragments of a broken cylindrical structure [17]. Extremal contours and discontinuities are salient features for localisation purposes. To this end, the line fitting is usually

applied on both side of the imaged cylinder axis for each set of classified contours. But in a complex environment, if many pixels of one of the two sets are occluded, the classification of apparent contours may fail, the resulting pose determination is then inaccurate or intractable. The current work aims at providing cylinder modeling and fitting for the overall apparent contours with the objectives of avoiding a tricky classification and to get a more robust results in presence of outliers. Finally, we expect this work bring contributions to the recovery and decoupling of the dof constrained to by visual tasks in robotics.

### B. Related work

In the early 90s, shape from contour approaches have been developed in an attempt to determine constraints on a 3-D scene structure based on assumptions about the shape. The understanding of the relations between image contours geometry, the shape of the observed object and the viewing parameters is still a challenging problem and it is essential that special shapes are not represented by freeform surfaces without regard to their special properties, but treated in a way more appropriate to their simple nature. Explicit relations from occluding contours to model a curved three-dimensional object have been presented for generalized cylinders (GC), straight homogeneous generalized cylinders (SHGC) or surfaces of revolution (SOR) ([2], [4], [9], [10], [16]). More recent works are based on the image contour of a cylinder cross-section. Puech *et al.* [11] used the image of two cross-sections to locate a straight uniform generalized cylinder in 3-D space and Shiu and Huang [14] solve the problem for a finite and known cylinder height, that is for 5 dof. Huang *et al.* [7] solve the pose determination of a cylinder through a reprojection transformation which may be viewed as a rectification. The computed transformation brings the camera optical axis to perpendicularly intersect the cylinder axis, which is then parallel to one of the two image axes. The new image (called "canonical" image) is a symmetrical pattern which simplifies the pose computation. It is an interesting method which provides an analytical solution, including the recovery of the height of the cylinder. However, it requires a prior image transformation and errors for estimating the reprojection transformation may lead to a significant bias in the contours location of the resulting canonical image and consequently to the pose parameters. In a similar way, Wong *et al.* [18] take advantage of the invariance of surfaces of revolution (SOR) to harmonic homology and have proposed to recover the depth and the focal length (by assuming that the principal point is

C. Doignon and M. de Mathelin are with the LSIT (UMR ULP-CNRS 7005), University of Strasbourg, Boulevard Brant, 67412 Illkirch, France.  
e-mail: {name}@lsiit.u-strasbg.fr

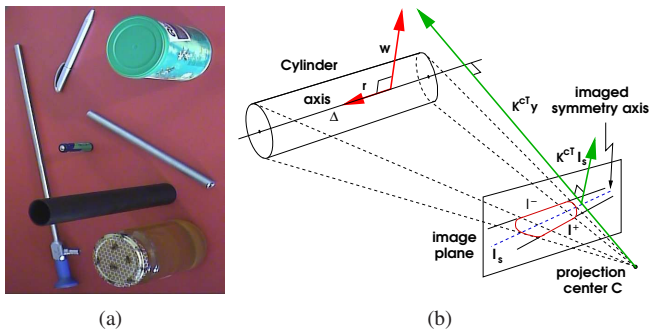


Fig. 1. (a) Some cylindrical objects: laparoscope, pen, honey pot, black plastic tube, jar of herbal tea, metallic pipe and cell. (b) A circular cylinder and its perspective projection  $P^c = K^c P$ . The backprojection of apparent lines  $(I^-, I^+)$  is a pair of planes  $(P^c)^T I^-$  and  $(P^c)^T I^+$ , passing through the projection center. The image of the cylinder axis  $\Delta$  is the axis  $I_s$  of the harmonic homology  $H$  relating the two apparent lines.

located at the image centre and that the camera has a unit aspect ratio) from the resulting silhouette which exhibits a bilateral symmetry. It is also a rectification which brings the revolution axis to coincide with the  $y$ -axis of the image and if the image of a latitude circle of the SOR may be located, the orientation of the cylinder axis can also be retrieved. A single view metric reconstruction of SORs applied to the texture acquisition has been addressed by Colombo *et al.* [1] from the apparent contour and the visible segments of two distinct imaged cross-sections. The solution proposed by the authors requires the SOR scaling function to be extracted from points sampled on the apparent contour, via a rectification. This paper points out interesting geometric properties of SORs which are revisited in the current work, since in the case of circular cylinders there is no distinct cross-sections.

In this article, we provide a geometrical representation for straight homogeneous circular cylinders (SHCC), an important subclass of SORs for which any cross-section is circular with identical radius. We present a two-stage algorithm for the direct pose computation from a single view, given its overall apparent contour in the image.

The remainder is organized as follows. In the next section, the geometric modeling of cylindrical objects as well as their perspective projections are presented in the case of SHCCs. The final part of this section is dedicated to the conic-based fitting and pose computation methods. Experimental results are analyzed in section three and we present in section four the 3-D localization of surgical instruments used in the robotized laparoscopic surgery.

## II. PROPOSED APPROACH

In the first part of the current section, we present a new geometrical model for the class of SHCC objects with a unknown (or infinite) height using the Plückerian representation of its symmetry axis. Second and third paragraphs review geometrical properties of a cylinder while the two last paragraphs give details of the pose determination from the imaged quadric which fits the overall apparent contour.

### A. Geometric modeling of a SHCC

We begin with the two following observations: first, a circular cylinder  $\mathcal{C}$  with radius  $r_c$  can be defined as a set of circles  $c_i$  with equal radii such that their centers  $\tilde{M}_i$  belong to a common straight line  $\Delta$  perpendicular to the circle planes. Second, a circle may be seen as the real intersection of a sphere  $\mathcal{S}$  with a plane  $\pi$ . Given a plane defined by the vector  $\pi = (\mathbf{r}^T, -d)^T$  with  $\mathbf{r}$  the unit vector perpendicular to that plane and  $d$  the orthogonal distance to the origin of the camera frame, a point  $\tilde{M}_i$  with homogeneous coordinates  $(\tilde{M}_i = (\tilde{M}_i^T, 1)^T)$  is lying in that plane only if  $\pi^T \tilde{M}_i = 0$ . It follows that  $d = \mathbf{r}^T \tilde{M}$  for any point  $\tilde{M}$  in the plane. On the other hand, a sphere with radius  $r_c$  and center  $\tilde{M}_i$  can be represented by the following  $(4 \times 4)$  matrix  $S$  such that:

$$\mathbf{M}^T S \mathbf{M} = \mathbf{M}^T \begin{bmatrix} \mathbf{I} & -\tilde{M}_i \\ -\tilde{M}_i^T & \tilde{M}_i^T \tilde{M}_i - r_c^2 \end{bmatrix} \mathbf{M} = 0 \quad (1)$$

where  $\mathbf{I}$  is the identity matrix. Since the sphere's centre  $\tilde{M}_i$  is lying on the straight line  $\Delta$  with the direction  $\mathbf{r}$ , any point  $\tilde{M}_o$  on this line satisfies  $\tilde{M}_i = \lambda \mathbf{r} + \tilde{M}_o$  ( $\lambda \in \mathbb{R}$ ). With a pre-multiplication in both side of the previous equation with vector  $\mathbf{r}^T$ , an expression for the scalar  $\lambda$  is given by  $\lambda = \mathbf{r}^T (\tilde{M}_i - \tilde{M}_o)$  or  $\lambda = \mathbf{r}^T (\tilde{M} - \tilde{M}_o)$ , since  $d = \mathbf{r}^T \tilde{M}_i = \mathbf{r}^T \tilde{M}$ . This allows to substitute the vector  $\tilde{M}_i$  in equation (1) by  $\tilde{M}_i = \mathbf{r} \mathbf{r}^T \tilde{M} + (\mathbf{I} - \mathbf{r} \mathbf{r}^T) \tilde{M}_o$ , that is

$$S = \begin{bmatrix} \mathbf{I} & \mathbf{0} \\ -\tilde{M}_o^T & 1 \end{bmatrix} \underbrace{\begin{bmatrix} \mathbf{I} - \mathbf{r} \mathbf{r}^T & \mathbf{0} \\ \mathbf{0}^T & -r_c^2 \end{bmatrix}}_{Q_{co}} \begin{bmatrix} \mathbf{I} & -\tilde{M}_o \\ \mathbf{0}^T & 1 \end{bmatrix} \quad (2)$$

The previous expression can be thought as a change in position (with position vector  $\tilde{M}_o$ ) of the degenerate quadric  $\mathcal{C}$  represented by the singular matrix  $Q_{co}$ . Let us now define the vector  $\mathbf{w}$  such that  $\mathbf{w} = \mathbf{r} \times \tilde{M}_o = [\mathbf{r}]_{\times} \tilde{M}_o$ . The two vectors  $(\mathbf{r}, \mathbf{w})$  are the Plücker coordinates of the cylinder axis ( $\mathbf{r}^T \mathbf{w} = 0$ ) and this representation is an efficient tool to handle geometric transformations of lines. It is a suitable representation which does not rely on the cylinder's height. The above expression (2) can be easily written in a way to only involve  $\mathbf{r}$ ,  $\mathbf{w}$  and  $r_c$  as the cylinder parametrization:

$$\mathbf{M}^T \underbrace{\begin{bmatrix} [\mathbf{r}]_{\times} [\mathbf{r}]_{\times}^T & [\mathbf{r}]_{\times} \mathbf{w} \\ \mathbf{w}^T [\mathbf{r}]_{\times}^T & \|\mathbf{w}\|^2 - r_c^2 \end{bmatrix}}_{Q_c} \mathbf{M} = 0 \quad (3)$$

and using the identity  $\mathbf{I} - \mathbf{u} \mathbf{u}^T = [\mathbf{u}]_{\times} [\mathbf{u}]_{\times}^T = -[\mathbf{u}]_{\times}^2$  for any unit vector  $\mathbf{u}$ . The symmetrical matrix  $Q_c$  is defined up to a scale factor. It is a singular matrix, thus representing a degenerate quadric surface since the determinant is equal to  $\det(Q_c) = \det(Q_{co}) = -r_c^2 \det([\mathbf{r}]_{\times})^2 = 0$ .

### B. Perspective projection of a SHCC

The perspective projection of a quadric is a conic  $\mathcal{C}$  which is usually computed by means of the dual matrix  $Q_c^*$  of  $Q_c$  thanks to the famous Cayley-Hamilton theorem (see [6] for details). In the case of a degenerate quadric, the dual  $Q_c^*$  is not unique since  $Q_c (Q_c^*)^T = 0$  and components are quite hard to compute with high accuracy. Alternatively, the projection

of any point  $\tilde{\mathbf{M}}$  on the cylinder surface with coordinates  $(x, y, z)$  in the camera frame may be projected onto the image plane at  $\mathbf{m} = (u, v, 1)^\top$ , thus satisfying the following relationship  $z \mathbf{m} = \mathbf{P}^c \mathbf{M} = \mathbf{K}^c \mathbf{P} \mathbf{M} = [\mathbf{K}^c \mid \mathbf{0}] \mathbf{M}$  or conversely as

$$\mathbf{M} = z \begin{bmatrix} (\mathbf{K}^c)^{-1} \\ \mathbf{0}^\top \end{bmatrix} \mathbf{m} + [0 \ 0 \ 0 \ 1]^\top \quad (4)$$

when the  $z$ -axis is chosen parallel to the camera optical axis and  $\mathbf{K}^c$  is the matrix of intrinsic parameters. The substitution in equation (3) of the expression for  $\mathbf{M}$  in the above equation (4) leads to a second-order polynomial equation of the form  $A z^2 + 2B z + C = 0$ , with

$$\begin{cases} A = \mathbf{m}^\top (\mathbf{K}^c)^{-\top} [\mathbf{r}]_\times [\mathbf{r}]_\times^\top \mathbf{m} \\ B = \mathbf{m}^\top (\mathbf{K}^c)^{-\top} [\mathbf{r}]_\times \mathbf{w} \\ C = \|\mathbf{w}\|^2 - r_c^2 \end{cases} \quad (5)$$

The apparent contour ( $\gamma$ ) of a cylinder is a set of points which intersects the viewline and the image plane. It is the projection of a 3-D curve on the cylinder's surface referred to as the contour generator ( $\Gamma$ ). This means that one has to solve the above polynomial equation for a unique (double) solution that is, for a discriminant  $B^2 - AC$  equal to 0 and after some computations, it can be expressed as

$$\left(\frac{r_c B}{\sqrt{C}} + \mathbf{w}^\top (\mathbf{K}^c)^{-1} \mathbf{m}\right)^\top \left(\frac{r_c B}{\sqrt{C}} - \mathbf{w}^\top (\mathbf{K}^c)^{-1} \mathbf{m}\right) = 0. \quad (6)$$

If the scalar  $C \leq 0$ , the projection center  $C_c = (0, 0, 0, 1)^\top$  is located inside the cylinder (or on its surface, if  $C = 0$ ) and yields no real solutions for  $z$ . This can be easily seen with equation (3) since the quantity  $C_c^\top \mathbf{Q}_c C_c \leq 0$  in this case. We do not consider these special cases in the remainder, we rather focus this work on the more practical situation with real solutions. In the case of a circular cylinder with infinite height and a constant radius, equation (6) shows that the apparent contour is a set of two straight lines represented either with the pair of vectors  $\mathbf{1}^-$  and  $\mathbf{1}^+$  satisfying

$$\begin{cases} (\mathbf{1}^-)^\top \mathbf{m} \equiv \{(\mathbf{K}^c)^{-\top} (\mathbf{I} - \alpha [\mathbf{r}]_\times) \mathbf{w}\}^\top \mathbf{m} = 0 \\ (\mathbf{1}^+)^\top \mathbf{m} \equiv \{(\mathbf{K}^c)^{-\top} (\mathbf{I} + \alpha [\mathbf{r}]_\times) \mathbf{w}\}^\top \mathbf{m} = 0 \end{cases} \quad (7)$$

with  $\alpha = r_c / \sqrt{\|\mathbf{w}\|^2 - r_c^2}$ , or alternatively with the real  $(3 \times 3)$  matrix  $\mathbf{C} = \mathbf{1}^- \mathbf{1}^{+\top} + \mathbf{1}^+ \mathbf{1}^{-\top}$  satisfying  $\mathbf{m}^\top \mathbf{C} \mathbf{m} = 0$ . The latter is a rank-2 symmetrical matrix defined up to a scale factor and both representations are equivalent to model the apparent contour with 4 parameters.

### C. Direct pose computation

The aim of this paragraph is to present a new methodology for the pose determination of a cylinder. We look for the estimation of the Plücker coordinates  $(\mathbf{r}, \mathbf{w})$  of the cylinder axis satisfying the non-linear equation  $\mathbf{r}^\top \mathbf{w} = 0$ . That is, given the matrix  $\mathbf{K}^c$  of the camera intrinsics, the cylinder radius  $r_c$  and the matrix  $\mathbf{C}$ . In the next two paragraphs, we discuss about some interesting imaged properties and we present a linear algorithm for estimating the degenerate conic  $\mathbf{C}$  given the apparent contour ( $\gamma$ ) of the cylinder.

Starting from equations (7), the matrix  $\mathbf{C}$  can be related to the pose parameters since in one hand, we have

$$\begin{aligned} \mathbf{K}^{c\top} \mathbf{C} \mathbf{K}^c &\equiv \mathbf{K}^{c\top} (\mathbf{1}^- \mathbf{1}^{+\top} + \mathbf{1}^+ \mathbf{1}^{-\top}) \mathbf{K}^c \\ &\equiv (\alpha [\mathbf{r}]_\times - \mathbf{I}) \mathbf{w} \mathbf{w}^\top (\alpha [\mathbf{r}]_\times^\top + \mathbf{I}) \\ &\quad + (\alpha [\mathbf{r}]_\times + \mathbf{I}) \mathbf{w} \mathbf{w}^\top (\alpha [\mathbf{r}]_\times^\top - \mathbf{I}) \\ &\equiv \alpha^2 [\mathbf{r}]_\times \mathbf{w} \mathbf{w}^\top [\mathbf{r}]_\times^\top + \mathbf{w} \mathbf{w}^\top \\ &\equiv [\mathbf{r}]_\times \left( \alpha^2 \frac{\mathbf{w} \mathbf{w}^\top}{\|\mathbf{w}\|^2} + \frac{[\mathbf{w}]_\times [\mathbf{w}]_\times^\top}{\|\mathbf{w}\|^2} \right) [\mathbf{r}]_\times^\top \\ &\equiv [\mathbf{r}]_\times (\mathbf{I} - (1 - \alpha^2) \frac{\mathbf{w} \mathbf{w}^\top}{\|\mathbf{w}\|^2}) [\mathbf{r}]_\times^\top \\ &\equiv (\mathbf{I} - \mathbf{r} \mathbf{r}^\top - \mathbf{z} \mathbf{z}^\top) \\ &= [\mathbf{a} \quad \mathbf{z}_u \quad \mathbf{r}] \begin{bmatrix} 1 & 0 & 0 \\ 0 & 1 - \sigma^2 & 0 \\ 0 & 0 & 0 \end{bmatrix} \begin{bmatrix} \mathbf{a}^\top \\ \mathbf{z}_u^\top \\ \mathbf{r}^\top \end{bmatrix} \end{aligned} \quad (8)$$

with  $\mathbf{z} = \frac{\sqrt{1 - \alpha^2}}{\|\mathbf{w}\|} [\mathbf{r}]_\times \mathbf{w}$  and the unit vector  $\mathbf{z}_u = \mathbf{z} / \sigma$ . In the other hand, the SVD has the following expression

$$\mathbf{K}^{c\top} \mathbf{C} \mathbf{K}^c = \mathbf{U} \mathbf{D} \mathbf{U}^\top = \mathbf{U} \text{diag}(\lambda_1, \lambda_2, 0) \mathbf{U}^\top. \quad (9)$$

It is easy to see that  $\mathbf{U} = [\mathbf{a} \quad \mathbf{z}_u \quad \mathbf{r}]$  and

$$\sigma = \|\mathbf{z}\| = \sqrt{1 - \alpha^2} = \sqrt{1 - \frac{\lambda_2}{\lambda_1}}.$$

Finally,  $\mathbf{w} \equiv \mathbf{z}_u \times \mathbf{r} = \mathbf{a}$  and

$$\|\mathbf{z}\| = \sqrt{1 - \frac{r_c^2}{\|\mathbf{w}\|^2 - r_c^2}} \Rightarrow \|\mathbf{w}\| = r_c \sqrt{1 + \frac{\lambda_1}{\lambda_2}}. \quad (10)$$

### D. Imaged properties of SHCCs

The direct pose computation gives rise to important geometric properties we would like to point out herein. The attitude of a SHCC symmetry axis may be represented with the Plücker coordinates as it is for any 3-D straight line and gathered in the Plücker matrix  $\mathbf{L}$  of rank 2 or its dual  $\mathbf{L}^*$ :

$$\mathbf{L} = \begin{bmatrix} [\mathbf{w}]_\times & -\mathbf{r} \\ \mathbf{r}^\top & 0 \end{bmatrix}; \quad \mathbf{L}^* = \begin{bmatrix} [\mathbf{r}]_\times & -\mathbf{w} \\ \mathbf{w}^\top & 0 \end{bmatrix}. \quad (11)$$

The perspective projection of the SHCC symmetry axis is the image line  $\mathbf{l}_s$  defined by (see [6])  $[\mathbf{l}_s]_\times = \mathbf{K}^c \mathbf{P} \mathbf{L}_s (\mathbf{K}^c \mathbf{P})^\top$ , (with  $\mathbf{P}$  as the  $(3 \times 4)$  projection matrix  $\mathbf{P} = [\mathbf{I} \mid \mathbf{0}]$ ) and one may check that this leads to the simple equation

$$\mathbf{l}_s \equiv (\mathbf{K}^c)^{-\top} \mathbf{w}. \quad (12)$$

Since the vector  $\mathbf{l}_s$  is defined up to a scale, it represents the imaged symmetry axis and it does not depend on the magnitude of  $\mathbf{w}$ , thus it can be recovered whatever the radius is. Moreover, while apparent contours are not in correspondence with multiple views, it is the case for the imaged symmetry axes, providing an easy way to recover the 3-D location of the cylinder symmetry axis with only two views.

### E. A degenerate conic fitting

In this part, the apparent contour ( $\gamma$ ) of the cylinder serves as input data for a degenerate conic fitting. It is a more convenient approach than considering two separate lines fitting ( $l^-$  and  $l^+$ ) for which the apparent contour must be splitted into two sets of pixels on both side of the imaged cylinder axis before performing the features parametrization. This two-class classification is not an obvious task, especially when the limbs are partly occluded. By the way, we are expecting to get a more convenient estimation - skipping contour classification - with only one fitting for data coming from the overall apparent contour.

1) *A constrained least-squares estimation:* A linear approach to estimating the matrix  $C$  when solving  $\mathbf{m}^T C \mathbf{m} = 0$  is now detailed. To get an accurate solution, one must keep in mind that the singularity constraint must also be satisfied, hence expressing that  $C$  has only 4 free parameters, that is:

$$\mathbf{m}^T C \mathbf{m} = 0 \quad \text{subject to} \quad C = C^T \quad \text{and} \quad \det(C) = 0 \quad (13)$$

To this aim, a vector  $\mathbf{c} = (C_{11}, C_{12}, C_{13}, C_{22}, C_{23}, C_{33})^T$  of matrix entries is defined so as to get an homogeneous system

$$U_n \mathbf{c} = \mathbf{0} \quad (14)$$

subject to  $\|\mathbf{c}\| = 1$  and where the measurement matrix  $U_n$  is

$$U_n = \begin{bmatrix} u_1^2 & 2u_1v_1 & 2u_1 & v_1^2 & 2v_1 & 1 \\ u_2^2 & 2u_2v_1 & 2u_2 & v_2^2 & 2v_2 & 1 \\ \vdots & \vdots & \vdots & \vdots & \vdots & \vdots \\ u_n^2 & 2u_nv_n & 2u_n & v_n^2 & 2v_n & 1 \end{bmatrix}_{n \times 6} \quad (15)$$

for image points  $\mathbf{m}_i = (u_i, v_i, 1)^T$  on the apparent contour. With  $n > 4$ , it is possible that because of noise corruption, the matrix  $U_n$  actually has a rank greater than 4. With exactly  $n = 4$ , the rank of the  $(n \times 6)$  matrix  $U_n$  generally has a rank equal to 4. The solution of (14) in this case is  $\rho \mathbf{c}_1 + \mu \mathbf{c}_2$  where  $\rho$  and  $\mu$  are scalars and  $\mathbf{c}_1$  and  $\mathbf{c}_2$  are two singular vectors associated to the two smallest singular values of  $U_n$ . It is important to notice that this solution is an approximation when  $n > 4$ . To find a satisfactory solution of this deficient-rank homogeneous system, data are normalized and the rank is enforced to get a singular matrix  $C$ . This may be written as  $\det(\rho C_1 + \mu C_2) = 0$  where matrices  $C_1$  and  $C_2$  are built from vectors  $\mathbf{c}_1$  and  $\mathbf{c}_2$  respectively. Either the scalar  $\mu$  has a zero value, then the solution is given by the singular matrix  $C_1$ , or (what is of interest herein)  $\mu \neq 0$  then  $C_1$  is non-singular. In the latter case, scalars  $\rho$  and  $\mu$  satisfy  $\rho^2 + \mu^2 = 1$  so that  $\|\mathbf{c}\| = 1$ . This leads to a cubic polynomial equation in  $\alpha = -\rho/\mu$ , for which the solutions are the eigenvalues of the symmetric matrix  $C_2 C_1^{-1}$ . From the three real solutions,  $\alpha_1, \alpha_2$  and  $\alpha_3$ , we choose  $\alpha = \alpha_i$  which is satisfying

$$\alpha_i = \arg \min \|U_n \mathbf{c}\|^2. \quad (16)$$

**A robust solution:** The well-known least median of squares approach [13] has been carried out with samples of exactly  $n = 4$  points. Briefly, for a putative linear solution, the algebraic error is computed with every other point of the

apparent contour so as to integrate it for the final numerical solution or to reject it [12]. This random selection is repeated, since the number of samples is also computed by the algorithm and depends on the fraction of outliers, the sample size and the probability that ensures at least one sample is free from outliers. The selected solution associated to a set of image points is the one which integrates the maximum image points with the minimum algebraic error.

2) *An iterative numerical solution:* When an initial solution is available, the problem we tackle in this part is to reduce the noise effect since the previous linear solution assumed the noise to be a gaussian process. A numerical approach is always more efficient, that's why we wish to solve

$$\min_{\mathbf{c}} \sum_{i=1}^n w_i (\mathbf{m}_i^T C \mathbf{m}_i)^2 \quad \text{subject to} \quad \det(C) = 0 \quad (17)$$

To get a more resistant-noise solution, we used the M-estimator (method S1) provided by Torr and Murray in [15] (based on the iterative re-weighted least squares with the Huber's influence function) in order to find the solutions of (17). It is a well-suited approach since it has been designed for the robust estimation of the Fundamental matrix, a matrix which shares many properties of  $C$  except for the symmetry.

## III. RESULTS

### A. Results using simulated data

1) *Sensitivity w.r.t. noise:* First of all, several simulations have been conducted with Matlab Software to validate the proposed algorithms. The robustness has been examined by introducing a gaussian noise with zero mean and outliers (random points) in the data, that is, on the contours location. Typical values for a classical vision system have been considered. The focal length is set to 1200 pixels and the cylinder radius has been arbitrarily set to 15 mm. For various noise levels (with standard deviation  $\sigma = 0.5, 1.0, 1.5$  and  $2.0$  pixels), relative errors on the orthogonal distance  $\frac{\|\mathbf{w}\| - \|\mathbf{w}_{ref}\|}{\|\mathbf{w}_{ref}\|}$  (see Fig. 2a-b) together with relative angular errors (see Fig.2c-d) have been reported for the pose algorithm while the distance or the orientation is varying. To carry out these simulations, 500 viewpoints have been defined for which the pose parameters have been randomly selected (with limited range), satisfying  $\|\mathbf{r}\| = 1$  and  $\mathbf{r}^T \mathbf{w} = 0$ .

As expected, the pose parameters accuracy strongly depends on the distance and noise level. Moreover, when the orientation of the cylinder axis is close to  $90^\circ$  (that is, when the cylinder is quite parallel to the optical axis  $\mathbf{r} = (0, 0, \pm 1)^T$ ), all the pose parameters are very affected and relative errors have been reported only up to  $87^\circ$  for this reason. It is a degenerate configuration and other features should be used to compute the pose with consistency.

### B. Results with real images

Two cylindrical plastic tubes with markers sticked on their surfaces have been used for experiments. A set of 30 images with different viewpoints has been captured with a calibrated

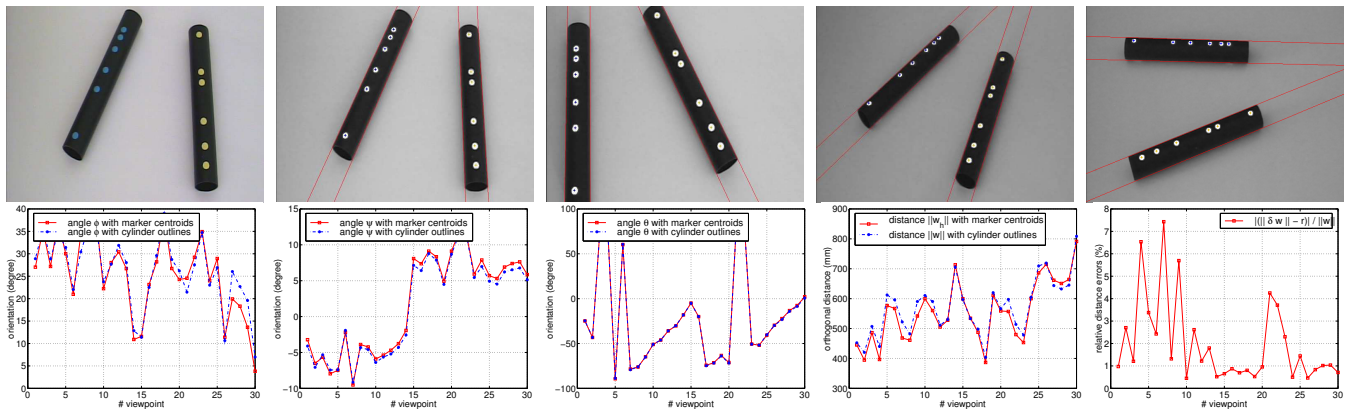


Fig. 3. (a) Image of the two plastic tubes with yellow and blue markers. (b) The robust fitting (in red) superimposed to the image for 4 viewpoints. (c-g) Comparison with the markers-based Haralick's method and the direct method based on apparent contours of a right circular cylinder. Angular (c-e) and distance (f) errors with real images on the top. While the orientation of the cylinder should be equal with and without markers, the norm of the vector subtraction  $\mathbf{w} - \mathbf{w}_h$  must differ with the radius  $r_c$  (g).

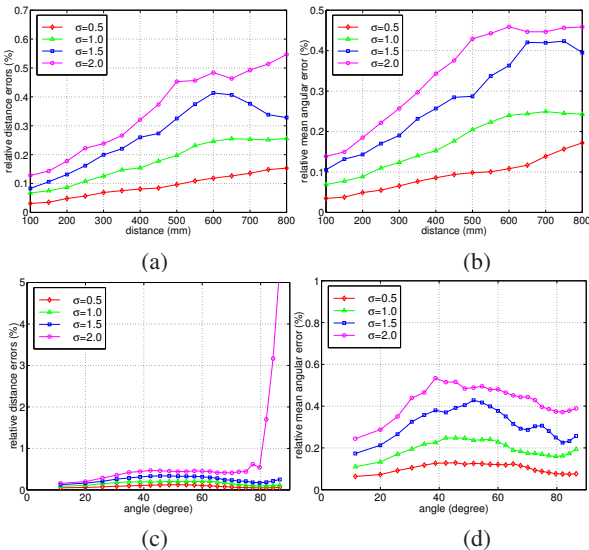


Fig. 2. The pose method accuracy in presence of noisy data for the determination of distance and orientation of the cylinder's axis when the orthogonal distance varies from 100 to 800 (a-b) mm and also when the orientation varies from 0 to  $90^\circ$  (c-d).

camera (4 viewpoints are shown in Fig.3a-b). Centroids of markers are such that we get a set of collinear object points in the axis direction. With this equipment, we have compared the pose computation from apparent contours of the cylinder ( $\mathbf{r}, \mathbf{w}$ ) with the direct pose method and the Haralick's method for the pose of a set of collinear points [5]. The latter method solves the orientation  $\mathbf{r}_h$  of the straight line supporting the points as well as a position vector  $\mathbf{t}_h$  (given the interpoint distances). We then compute the following cross-product  $\mathbf{w}_h = \mathbf{r}_h \times \mathbf{t}_h$  to get the Plückerian coordinates. Due to the relative position of these markers w.r.t. the cylinder axis, vectors  $\mathbf{r}$  and  $\mathbf{r}_h$  should coincide whereas the Euclidean norm of vector  $\delta\mathbf{w} = \mathbf{w} - \mathbf{w}_h$  should be equal to the cylinder radius  $r_c = 15$  mm. This experimental validation is depicted in Fig.3c-d for the orientation (angles  $\phi$  and  $\psi$ ) of the rotation

axis, in Fig.3e for the inclination of the interpretation plane w.r.t. to the optical axis (angle  $\theta$ ) and in Fig.3f for the orthogonal distances. It is worth pointing out that orthogonal distances with the two kinds of features must differ with the radius  $r_c$  (Fig.3g) whereas the orientation of the cylinder should be equal with and without markers. The results show a good agreement and consistency for the orientation of the rotation axis. However, results about relative distance error are not as good as expected. This error is 3.1 % in average, but for several viewpoints it is significant (up to 7.6 %).

#### IV. APPLICATION

The application of concern is in the field of the computer-assisted surgery, especially the intra-operative image-guidance in minimally invasive surgery (MIS) for which an attractive technique is the robotized laparoscopy<sup>1</sup>. Our research aims at providing new functionalities to these systems by using visual tracking and servoing techniques in order to perform semi-autonomous tasks. One of these functionalities is the visual tracking of surgical instruments. To do so, one has to overcome many difficulties like the non-uniform and time-varying lighting conditions and the moving background (due to breathing and heart beating). In laparoscopic surgery, most of surgical instruments have cylindrical parts (see Fig.4). Prior researchs involving endoscopic images with laparoscopes have been conducted in the field of color image segmentation [3]. Once regions have been segmented, the region boundaries are ordered and used to perform the contours fitting. With these data, the least-median of squares method for the degenerate-conic has been carried out for solving the pose. With the calibrated and distortion-corrected endoscope used in the experiments, the 3-D localization of the two moving surgical instruments in Fig.4 (bottom) have been done with success for more than 300 successive images of the abdominal cavity of a pig.

<sup>1</sup>Laparoscopic surgery is a surgical procedure where small incisions are made in the body (usually, the abdomen) in order to introduce, through trocars, surgical instruments and the endoscopic optical lens of a camera.

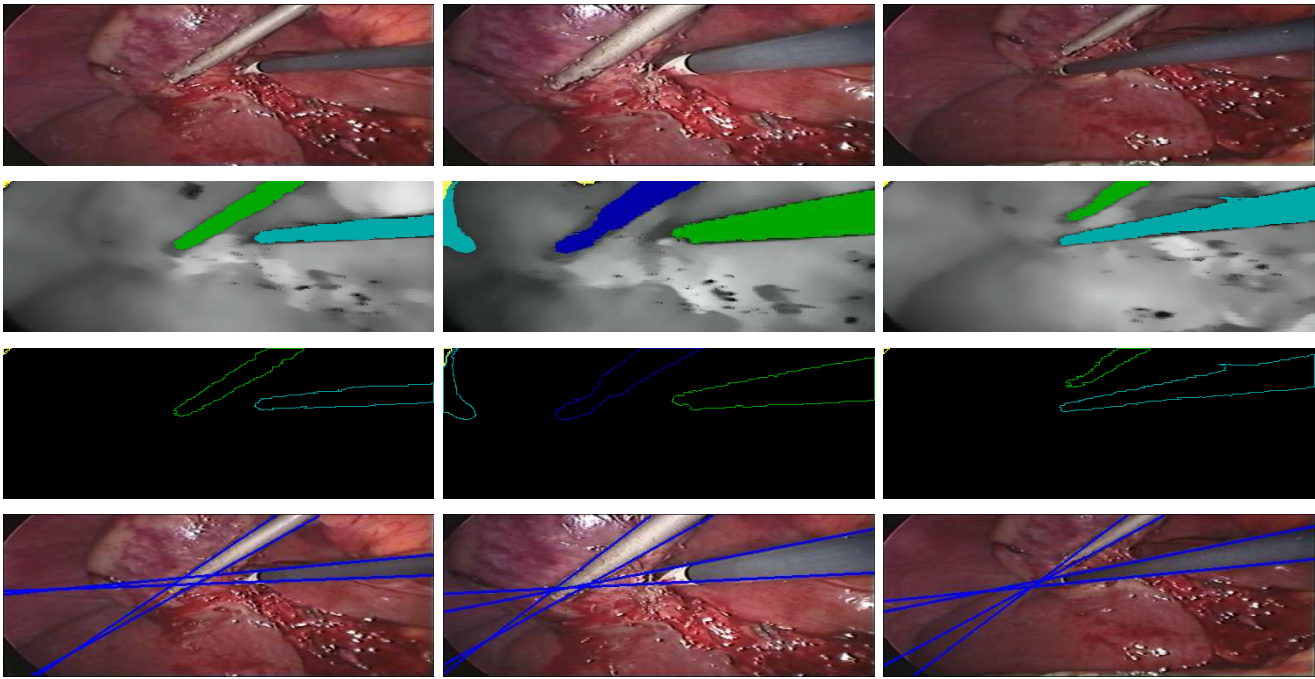


Fig. 4. Segmentation of three endoscopic images of surgical instruments in the abdominal cavity. (top) Original (de-interlaced) images. (top-middle) Region growing of selected regions in the joint hue saturation HS-image. (bottom-middle) Region boundaries. (bottom) The degenerate conic fitting (in blue) with the overall apparent contour of the two cylindrical instruments.

## V. CONCLUSION

We have addressed the problem of estimating the pose of a straight homogeneous circular cylinder from a single perspective view of its surface outlines. To tackle this problem, we have firstly proposed a geometric model with a singular matrix composed with the Plücker coordinates of the symmetry axis and the cylinder radius. We have presented a degenerate conic-based fitting approach and we have provided both a closed-form solution and a numerical minimization. Experiments (simulations and real endoscopic images with laparoscopes) and comparison with a marker-based pose estimation gave satisfactory results concerning the orientation (3 dof), however it also revealed that the distance estimation should be improved (relative mean distance error is about 3 %). We have also shown that the imaged symmetry axis was independent of the distance and of the cylinder radius, providing a reliable image feature to track in the parameter space. In the future, the visual 3-D tracking of surgical instruments, including the tip, will be investigated as a new step towards an autonomous (task-based) endoscopic vision system for the minimally invasive surgery.

## REFERENCES

- [1] C. Colombo, A. Del Bimbo, and F. Pernici. Metric 3d reconstruction and texture acquisition of surfaces of revolution from a single uncalibrated view. *IEEE Transactions on PAMI*, 27(1):99–114, 2005.
- [2] M. Dhome, J.-T. Lapreste, G. Rives, and M. Richetin. Spatial localization of modelled objects of revolution in monocular perspective vision. In *Proceedings of ECCV*, Antibes, France, 1990.
- [3] C. Doignon, P. Graebbling, and M. de Mathelin. Real-time segmentation of surgical instruments inside the abdominal cavity using a joint hue saturation color feature. *Real-Time Imaging*, 11:429–442, 2005.
- [4] M. Ferri, F. Mangili, and G. Viano. Projective pose estimation of linear and quadratic primitives in monocular computer vision. *CVGIP: Image understanding*, 58(1):66–84, July 1993.
- [5] R.-M. Haralick and L.-G. Shapiro. *Computer and Robot Vision*, volume 2. Addison-Wesley Publishing, 1992.
- [6] R. Hartley and A. Zisserman. *Multiple view geometry in computer vision*. Cambridge Univ. Press, 2000.
- [7] J.-B. Huang, Z. Chen, and T.-L. Chia. Pose determination of a cylinder using reprojection transformation. *Pattern Recognition Letters*, 17:1089–1099, 1996.
- [8] D. Knossow, J. Van de Weijer, R. Horaud, and R. Ronfard. Articulated-body tracking through anisotropic edge detection. In *Int'l Workshop on Dynamical Vision, ECCV 2006*, Graz, Austria, May 2006.
- [9] D.-J. Kriegman and J. Ponce. On recognizing and positioning curved 3-d objects from image contours. *IEEE Trans. on PAMI*, 12(12), 1990.
- [10] J. Ponce, D. Chelberg, and W. Mann. Invariant properties of straight homogeneous generalized cylinders and their contours. *IEEE Trans. on Pattern Analysis and Machine Intelligence*, 11(9):951–966, 1989.
- [11] W. Puech, J.-M. Chassery, and I. Pitas. Cylindrical surface localization in monocular vision. *Pattern Recognition Letters*, 18:711–722, 1997.
- [12] P.L. Rosin. Robust pose estimation. *IEEE Transactions on Systems, Man, and Cybernetics (PartB)*, 29(2), April 1999.
- [13] P. Rousseeuw and A. Leroy. *Robust Regression and Outlier Detection*. Wiley, NY, 1987.
- [14] Y.-C. Shiu and C. Huang. Pose determination of circular cylinders using elliptical and side projections. In *Int'l Conf. on Systems Engineering*, pages 265–268, Dayton, OH, USA, August 1991.
- [15] P.H.S. Torr and D.W. Murray. The development and comparison of robust methods for estimating the fundamental matrix. *Int'l Journal of Computer Vision*, 24(3):271–300, 1997.
- [16] F. Ulupinar and R. Nevatia. Shape from contour: Straight homogeneous generalized cylinders and constant cross-section generalized cylinders. *IEEE Trans. on PAMI*, 17(2):120–135, 1995.
- [17] S. Winkelbach, R. Westphal, and T. Goesling. Pose estimation of cylindrical fragments for semi-automatic bone fracture reduction. In *DAGM Symposium on Pattern Recognition*, pages 566–573, 2003.
- [18] K.-Y. Wong, P.-R.-S. Mendonça, and R. Cipolla. Reconstruction of surfaces of revolution from single uncalibrated views. *Image and Vision Computing*, 22:829–836, 2004.